

Dwarf galaxies in observed and simulated galaxy clusters*

Ludwig Biermann Award Lecture 2011

T. Lisker**

Astronomisches Rechen-Institut, Zentrum für Astronomie der Universität Heidelberg, Mönchhofstraße 12-14, D-69120 Heidelberg, Germany

Received 2012 Apr 7, accepted 2012 Apr 11

Published online 2012 Jun 15

Key words galaxies: clusters: general – galaxies: dwarf – galaxies: evolution – galaxies: structure

Galaxy clusters are populated by thousands of low-mass galaxies, with hundreds of them already within stellar masses of $10^8 \leq M_* \leq 10^{9.5} M_\odot$ and magnitudes of $-16 \leq M_r \leq -19$ mag. While objects in this regime are commonly termed “dwarfs”, they are not as faint and diffuse as many of the known Milky Way satellites. Their observed complexity, particularly regarding the dominant early-type dwarf population, is still poorly understood and requires models and simulations of environmental influence on dwarfs. Studying cluster dwarf galaxies at the current time is motivated by two facts: (i) for nearby clusters, multicolour observational samples exist that are complete in the above luminosity range and cover a substantial portion of the cluster; (ii) state-of-the-art semi-analytic models based on high-resolution N-body simulations, reaching down to dwarf masses, have recently become available. Here I show how comparisons of models and observations can serve as a tool for studying the evolutionary history of low-mass galaxy populations in today’s clusters.

© 2012 WILEY-VCH Verlag GmbH & Co. KGaA, Weinheim

1 Introduction

We tend to believe that the optical appearance and distribution of galaxies in a given environment tells us something about its stage of evolution. As an example, the Coma cluster shows almost exclusively “red and dead” galaxies from its core to its outskirts, while lots of spiral and star forming galaxies can be seen in the Hercules cluster, along with a noticeable number of galaxy interactions (Fig. 1). Hercules is known to consist of at least three galaxy groups that are coming together just “now”, whereas Coma is considered to be a more evolved system in an advanced evolutionary stage (e.g. Chiboucas et al. 2011; Petropoulou et al. 2011).

What defines the evolutionary proper time of an environment? Galaxy groups with similar galaxy numbers can differ significantly in their compactness, their early-type fractions and their intra-group medium (e.g. Tully & Trentham 2008; Torres-Flores et al. 2009). The Coma cluster, while being evolved in its galaxy content, has noticeable irregularities in its X-ray morphology (White et al. 1993). The Virgo cluster has a more centrally peaked X-ray profile but less evolved galaxies with significant substructure in their distribution (Schindler et al. 1999). In short, the diversity of environments is large, yet still poorly understood.

One way to study environmental properties and evolution is through comparisons of observed groups and clusters with their counterparts in astrophysically motivated semi-

analytic models. Limited by the resolution of the underlying cosmological N-body simulations, only recent models reach significantly into the regime of low-mass galaxies (“dwarfs”) while at the same time representing a large volume encompassing many galaxy clusters and groups. Here I present comparisons of the real and the model universe with focus on low galaxy masses, using the semi-analytic model of Guo et al. (2011), which is the first such model built on the high-resolution Millennium-II simulation (Boylan-Kolchin et al. 2009). I will illustrate advantages, but also limitations, of such comparisons, showing how models can be used to gain insight into real clusters and their galaxies, but also how mismatches between model and observations may lead to future improvements. Large parts of this article are taken from Lisker (2011) since this provided the backbone of my Ludwig Biermann Award lecture.

Diffuse, low-mass galaxies are ideal probes of the characteristics and evolutionary history of an environment, as they are not only abundant but also vulnerable to external influence like ram pressure and tidal forces, due to their shallow potentials. Given that many dwarfs, particularly those seen as early types today, entered the cluster many gigayears ago and have been exposed to tides and ram pressure ever since, we can consider them as fossils that carry an imprint of the past environmental influence. To decipher this fossil record, we need to gain a thorough understanding of their systematic characteristics at present, and combine this with models and simulations.

The recent years have revealed a broad diversity of dwarf galaxy properties. Adding to the known variety of late-type galaxies – bulgeless spirals, irregulars with dif-

* Partly based on observations collected at the European Organisation for Astronomical Research in the Southern Hemisphere, Chile (programme 077.B-0785).

** Corresponding author: tlisker@ari.uni-heidelberg.de

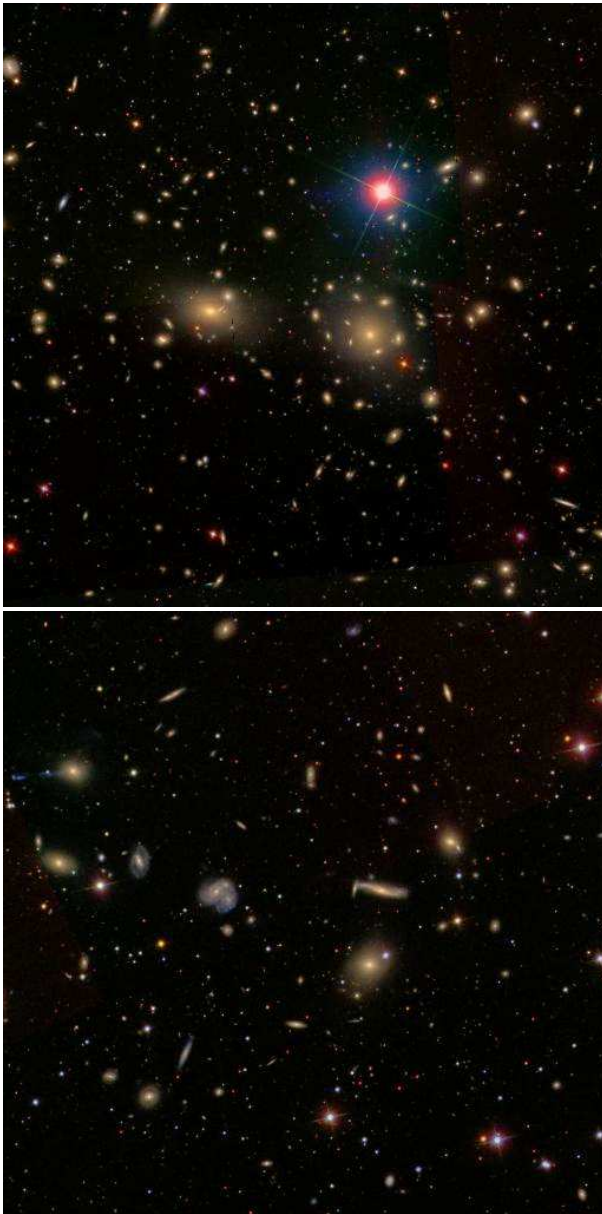


Fig. 1 The Coma galaxy cluster (*top*) and Hercules galaxy cluster (*bottom*), imaged by the Sloan Digital Sky Survey (SDSS, Abazajian et al. 2009).

fuse low-level star formation, and blue compact dwarfs with starbursts on top of an old population – passive early-type dwarfs, the most abundant galaxy population of clusters, have been shown to populate various different subclasses (Janz et al. 2012; Lisker et al. 2007). Those with weak disk substructure, like spiral arms and bars, may either be partially transformed disk galaxies, or they may be a natural continuation of normal lenticular (S0) galaxies. The seemingly “normal” early-type dwarfs without any of the previous features still show a pronounced difference in their distribution and stellar populations depending on whether or not they host a compact stellar nucleus in their center. A popular scenario connects these nuclei to an intriguing class of objects, the so-called ultra-compact dwarf (UCD) galax-

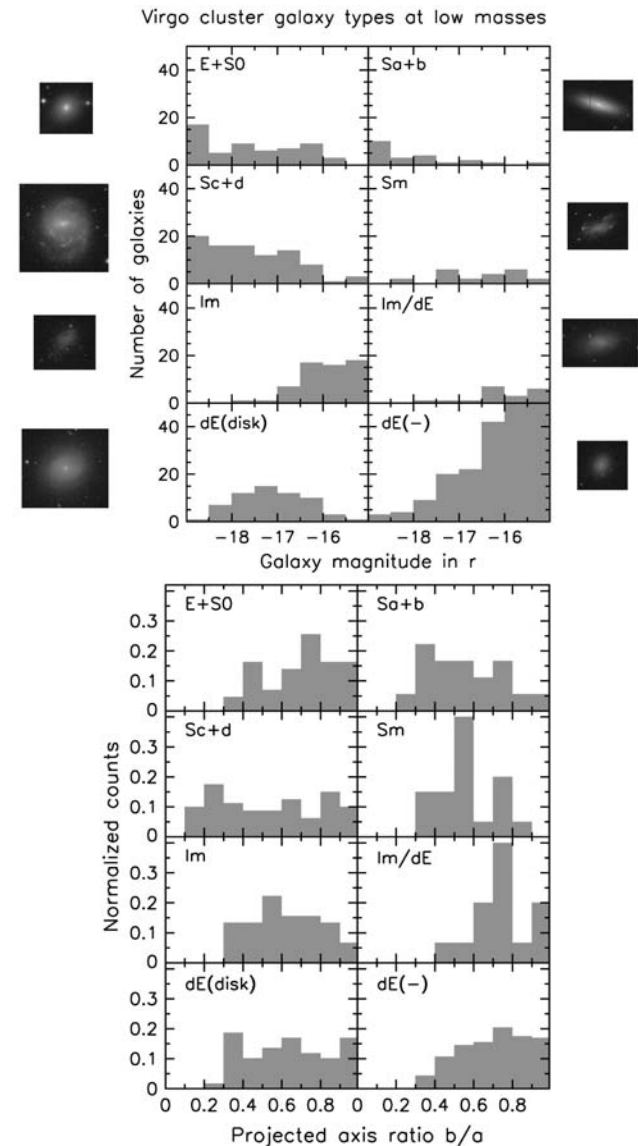


Fig. 2 Distribution of *r*-band magnitudes (*top*) and projected axis ratios (*bottom*) for the galaxy types in the Virgo cluster, using both certain and possible members according to Binggeli et al. (1985) and Lisker et al. (2007). Example images from SDSS are shown for each type. Magnitudes and axis ratios are from Janz & Lisker (2008) and Meyer et al. (in prep.).

ies (Hilker et al. 1999), which may be leftover nuclei from tidally destroyed host galaxies.

In the future, with facilities like the European Extremely Large Telescope, studies of resolved stellar populations at distances beyond the Virgo cluster will set a new level for investigating the stellar content of galaxies in detail, and will provide the knowledge to optimize integrated studies of stellar populations at much larger distances, probing more diverse environments and a larger lookback time, in order to virtually “watch” galaxies evolve.

2 Galaxy types at low luminosities

One is sometimes led to think that the famous Hubble sequence of galaxy types – from ellipticals (E) over lenticulars (S0) to early spirals (Sa/b) and late spirals (Sc/d) – is only valid for “normal” galaxies, whereas dwarf galaxies are either dwarf ellipticals (dE) or irregulars (Im). Figure 2 illustrates that this is a far too simplified picture. At low stellar masses and faint magnitudes ($M_r > -19$ mag), almost all galaxy classes coexist; it is merely a debate over semantics which of them are called dwarfs. It may seem surprising at first glance that a significant number of E/S0 galaxies is present at these magnitudes – but as one can see in the example picture, these clearly have a higher central surface brightness than the diffuse dEs. Spiral galaxies, especially of the later types, are frequently found at these magnitudes as well, while the actual irregulars only begin to be present fainter than $M_r \approx -17$ mag.

Towards the central cluster region, late-type galaxies appear in smaller and smaller numbers, and early types, particularly dEs, dominate. It is therefore commonly believed that an interplay of mechanisms transform late-type, disk-dominated galaxies into dEs. However, the figures already show that the frequently heard statement that dEs are formed out of irregulars does not work for the bright end of dEs, since the number of irregulars (at least at the present day) at these magnitudes is very small. The contrast even increases when considering the fact that present-day irregulars are still forming stars and have thus built up stellar mass for a longer time than dEs did, i.e. they even have *increased* their luminosity in the last gigayears as compared to the dEs (cf. Boselli et al. 2008).

While irregulars are relatively thick or fluffy objects, with axis ratios often larger than $b/a = 0.5$ (Binggeli & Popescu 1995), brighter late-type galaxies (Sc/Sd) show a more pronounced disk structure in optical images, and have smaller axis ratios (Fig. 2, bottom). It is thus not trivial to “transform” such galaxies into the apparently spheroid-like dEs. Moreover, as I outline below, it may be too simple to regard all early-type dwarfs as small, diffuse ellipticals. A subclass of dwarf lenticulars had already been defined by Sandage & Binggeli (1984), based on indications for disk components. For the purpose of simplification, I subsume them as dEs hosting disks, thus using the name “dE” for all early-type dwarf galaxies.

3 Disks and rotation in early-type dwarfs

3.1 Kinematics

The presence of significant rotation in some early-type dwarfs (Bender & Nieto 1990) raised the question whether or not all of them show this characteristic. Several studies confirmed that many, but apparently not all early-type dwarfs are consistent with rotational flattening or even rotational support, usually interpreted as being indicative of

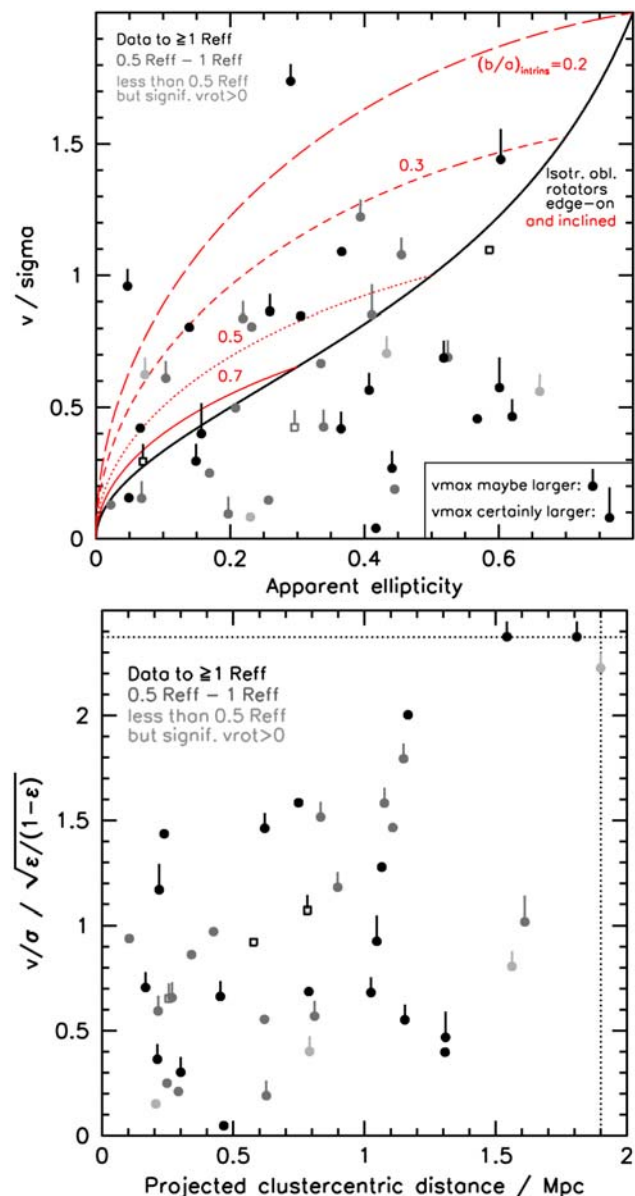


Fig. 3 Published kinematic data for Virgo cluster early types with $-19 \leq M_r \leq -16$ mag (Chilingarian 2009; Pedraz et al. 2002; Simien & Prugniel 2002; Toloba et al. 2011; van Zee et al. 2004). Maximum rotational velocity and (central or average) velocity dispersion were determined differently by different authors. The radial extent of the data was inferred by visual inspection of the published figures for each galaxy, and was compared to the half-light semimajor axis (R_{eff}) in r from Janz & Lisker (2008). When the radial extent is less than $0.5R_{\text{eff}}$, a galaxy is only included if it shows significant rotation. If the visual inspection indicated that the rotation curve is still rising beyond its coverage, this is denoted by an upward-pointing line attached to the data point. The top panel shows apparent ellipticity versus v/σ , compared to the theoretical curve from Binney (1978) for a rotationally flattened isotropic oblate spheroid viewed edge-on (black solid line) and under different inclinations (red lines, with intrinsic thicknesses as labeled). In the bottom panel, v/σ has been divided by the curve’s analytical approximation $\sqrt{\epsilon/(1-\epsilon)}$ and is shown versus projected clustercentric distance. Data points lying beyond the diagram boundaries have been put onto the dotted lines.

their former disk nature (Chilingarian 2009; De Rijcke et al. 2005; Simien & Prugniel 2002; Toloba et al. 2011; van Zee et al. 2004, e.g.). The current census of published kinematics for Virgo cluster early-type dwarfs is shown in Fig. 3, compared to the theoretical curve from Binney (1978) for a rotationally flattened isotropic oblate spheroid viewed edge-on and under different inclinations. The figure contains 39 dEs (filled circles) and 3 faint E/SOs (squares), yet only for 19 dEs, the available data reaches the half-light radius (black symbols). For most galaxies, visual inspection of the published rotation curves suggests that they may still be rising beyond the data coverage (indicated by the upward lines). Our knowledge of dE kinematics must therefore be regarded as rather incomplete.

Nevertheless, the available data clearly show that the vast majority of dEs show measurable rotation, in many cases reaching the curve for rotationally flattened oblate spheroids¹ or even exceeding it. While there are some dEs that seem to be flattened by anisotropy rather than rotation, a robust conclusion from the published kinematics is only possible for one object: VCC 1261 (at an ellipticity of 0.42), one of the brightest Virgo dEs ($M_r = -18.50$ mag). It is located at a projected clustercentric distance of 0.46 Mpc, thus being in the inner (projected) part of the cluster. Most of the other slow-rotating dEs are also found there (Fig. 3, bottom), while those with substantial rotation are distributed over all distances. The objects with the largest ratios of rotational velocity to dispersion are found in the cluster outskirts, probably being the least affected by environment (Toloba et al. 2009).

The structural transformation from disk galaxies to small spheroids by the combined effect of a strong tidal field and repeated encounters with massive galaxies, known as “galaxy harassment” (Moore et al. 1996), is frequently quoted to explain the origin of dEs. However, beside the extreme case of creating a dynamically hot system fully supported by random motion (simulation run GAL6 of Mastropietro et al. 2005), the remnants of this process can span a large range in kinematical properties (Mastropietro et al. 2005). Only in the very core region of the cluster can strong cases of structural reshaping occur (Smith et al. 2010). One thus needs to consider the fact that “harassment” is not a process with a fixed outcome (an ellipsoidal dwarf), but that there is a continuum of tidal influence that a low-mass cluster galaxy can experience.

3.2 Weak spiral arms

The weak spiral features seen in some dEs (Fig. 4) are clear signs of dynamically cold stellar disks (Lisker & Fuchs 2009). Are these the remainders of the progenitor late-type spirals? Indeed, Mastropietro et al. (2005) found in their simulations of the tidal influence on low-mass cluster galaxies that none of the stellar disks are completely destroyed.

¹ Note that this curve had not been derived for the diffuse dEs with their exponential surface brightness profiles; it therefore only serves as approximate reference.

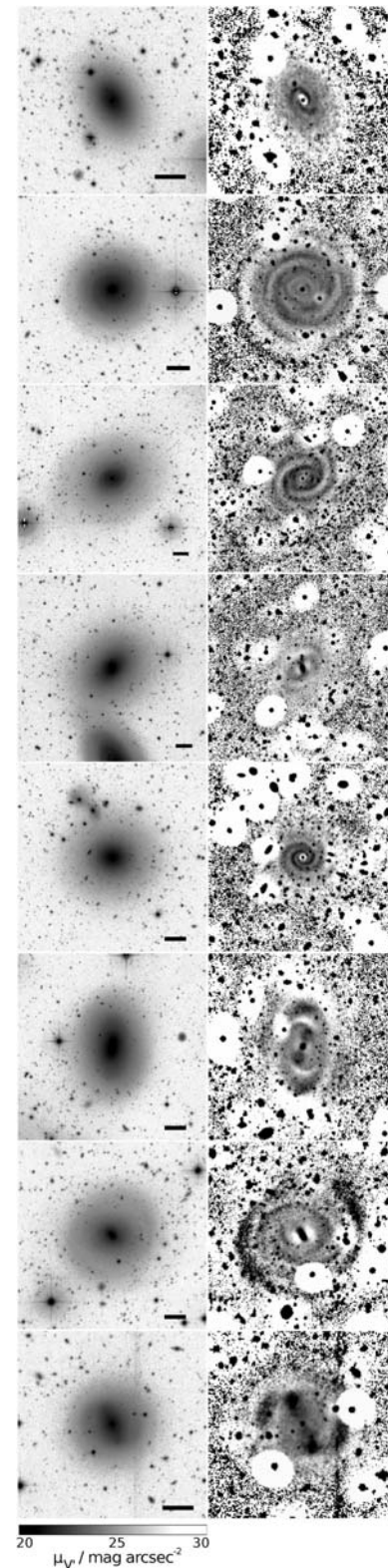


Fig. 4 Images taken with the white filter of ESO 2.2m/WFI, and their corresponding unsharp masks for Virgo dEs VCC 216, 308, 490, 523, 856, 1010, 1695, 1896 (top to bottom). A V -band equivalent surface brightness scale is provided at the bottom. The unsharp mask was created with elliptical Gaussian smoothing and a radially increasing kernel. The black scale bar corresponds to 2 kpc for the image and 1.33 kpc for the unsharp mask.

Tutukov & Fedorova (2006) argued that close passages of galaxies in clusters can occur at relative velocities sufficiently low to induce spiral structure. The simulation results of Tutukov & Fedorova, while being carried out for more massive galaxies, look very similar to the dE spirals shown here.

Most of these dEs show a two-component structure in our deep optical images (Lisker et al. 2009b), with the disk extending beyond what appears to be a low-Sérsic- n bulge-like component. This raises the question whether early-type dwarfs with disk galaxies really are (partially) transformed late-type disk galaxies falling into the cluster, or whether they simply form a continuum in mass with normal S0/spiral galaxies. An additional finding that might become relevant for future models and interpretations of these galaxies is the different visible extent of the spiral structure: While in some cases, the spiral structure appears confined to the inner region (VCC 216, 856), it extends across the whole galaxy in other cases, even dominating the galaxy light at large radii (VCC 308, 1695).

4 Close dwarf-dwarf passages

Following the study of Tutukov & Fedorova (2006) and using cluster galaxies in a “model universe”, provided by the semi-analytic model of Guo et al. (2011) and the Millennium-II simulation (Boylan-Kolchin et al. 2009), I now try to assess whether the number of close dwarf-dwarf passages could be responsible for the observed number of dEs with weak spiral arms. From analytical considerations, Tutukov & Fedorova estimate that there must be a non-negligible number of close passages of galaxies with relatively low velocities. The lower the relative velocity, the more time the galaxies spend close to each other, and the stronger the tidal influence can be. The study of Tutukov & Fedorova (2006) shows that “grand-design”, tightly wound spirals of different strength and lifetime are induced, depending on the parameter configuration.

I consider model galaxies of Guo et al. (2011) with $3 \times 10^8 \leq M_* \leq 5 \times 10^9 M_\odot$ in the four clusters with $2.4 \times 10^{14} \leq M_{\text{vir}} \leq 4.0 \times 10^{14} M_\odot$. Three different mass ranges of potential perturbers are defined: range “A” (average) for perturbers between 0.4 and 2.5 times the target mass (± 1 mag for equal M/L), range “L” (low) for perturbers between 0.1 and 0.4 times the target mass ($+2.5$ to $+1$ mag), and range “H” (high) for perturbers between 2.5 and 10 times the target mass (-1 to -2.5 mag). Low-mass perturbers will only be considered when they reach smaller distances, as the expected tidal effect is smaller. Conversely, high-mass perturbers will only be taken into account at somewhat larger distances, since a very close passage of a higher mass object could have a stronger, potentially disruptive effect on the target.

Based on Tutukov & Fedorova’s study, I estimate that the minimum perturber distance should be 10 kpc. Since this

minimum distance can only be observed during a short moment, potential perturbers need to be looked for in a larger radius around the target galaxy. As the time between two snapshots of the Millennium-II simulation at low redshift is 270 Myr, a galaxy’s motion cannot be accurately followed. Instead, I simply derive an estimate for the number of perturbers from the number of neighbour galaxies present in the second-last simulation snapshot, which I take to be “today”.² Given that the distance to a perturber with a (constant) relative velocity of 300 km s^{-1} can change by up to ~ 80 kpc within the 270 Myr, the following simple approach is applied for counting neighbours:

- In mass range A: (i) all neighbours within 20 kpc, (ii) 50 % of neighbours between 20 and 40 kpc;
- in mass range L: (i) all neighbours within 10 kpc, (ii) 50 % of neighbours between 10 and 20 kpc;
- in mass range H: (i) 50 % of neighbours within 20 kpc, (ii) all neighbours between 20 kpc and 40 kpc, (iii) 50 % of neighbours between 40 and 80 kpc;

with relative velocities of less than 300 km s^{-1} , and within less than $2R_{\text{vir}}$ from the cluster center.

The distributions of closest neighbours for the low-mass model galaxies are shown in Fig. 5, separately for the three different mass ranges. Counting potential perturbers as outlined above yields the following numbers:

- In mass range A: (i) all **2** neighbours within 20 kpc, (ii) 50 % of 14 neighbours between 20 and 40 kpc = **7** objects;
- in mass range L: (i) all **4** neighbours within 10 kpc, (ii) 50 % of 2 neighbours between 10 and 20 kpc = **1** object;
- in mass range H: (i) 50 % of 3 neighbours within 20 kpc = **1.5** objects, (ii) all **4** neighbours between 20 kpc and 40 kpc, (iii) 50 % of 8 neighbours between 40 and 80 kpc = **4** objects,

This leads to 23.5 perturbers, or on average 6 per cluster (since 4 clusters were used). When assuming a lifetime of induced features of ~ 500 Myr, i.e. ~ 2 snapshots of the simulation, there could be about a dozen such tidally induced features visible in galaxies of the stellar mass range typical for the observed dEs with disks. Only in few cases did the model galaxies enter a larger halo less than 3 Gyr ago, i.e. most of them should be representing early-type galaxies. There are 8 observed dEs with unambiguous spiral structure that are certain members of the Virgo cluster (Fig. 4), five of which also show bars, as well as four further galaxies with bars (Janz et al. 2012).

While the above analysis has been restricted to small relative velocities of less than 300 km s^{-1} , Fig. 6 shows that high relative velocities actually only occur in the central region of the cluster. Due to the high number density of galaxies there, close neighbours can pass each other with high speed. Outside of 0.5 virial radii, most close neighbours have relative velocities below 500 km s^{-1} .

² This is roughly the average of the lookback times to the Perseus and Coma clusters, and has been used in Weinmann et al. (2011) as well.

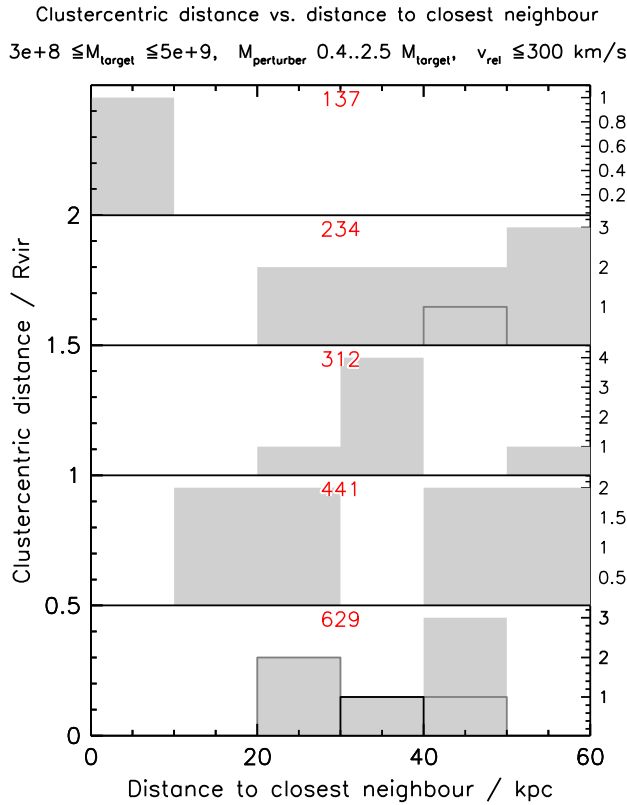


Fig. 5 (online colour at: www.an-journal.org) Distributions of distance to the closest neighbour, for intervals in clustercentric distance and model clusters with $2.4 \times 10^{14} \leq M_{\text{vir}} \leq 4.0 \times 10^{14} M_{\odot}$. Number counts are given on the right. Targets and neighbours are selected in stellar mass, mass ratio, and relative velocity as indicated in the plot. The grey shaded histogram shows all neighbours; the grey thin histogram indicates objects with at least one further neighbour in the parameter range shown; the black thin histogram indicates objects with more than one further neighbour. The red numbers denote the number of potential targets, i.e. all galaxies in the given stellar mass and distance range.

In order to check whether the model investigation can be representative for the Virgo cluster, the distribution of projected Virgo cluster galaxy neighbours was compared to the different projected distributions for the model clusters. Between 0.5 and 1 projected virial radii, the distributions are similar and the number of galaxies with close neighbours agree to within $\sim 30\%$ (assuming equal M/L for all galaxies). However, in the inner region from 0 to $0.5R_{\text{vir}}$, the model clusters clearly show a larger fraction of closer neighbours than Virgo. The number of total galaxies is lower by a factor of more than 3 in the Virgo cluster as compared to the model cluster average, and the number of galaxies with close neighbours is lower by a factor of more than 5. This may seem odd, given the good agreement outside of $0.5R_{\text{vir}}$ – however, the strong discrepancy in the central number of galaxies between Virgo and the model clusters was already reported by Weinmann et al. (2011). The mismatch is illustrated in Fig. 7, which compares an SDSS image of the

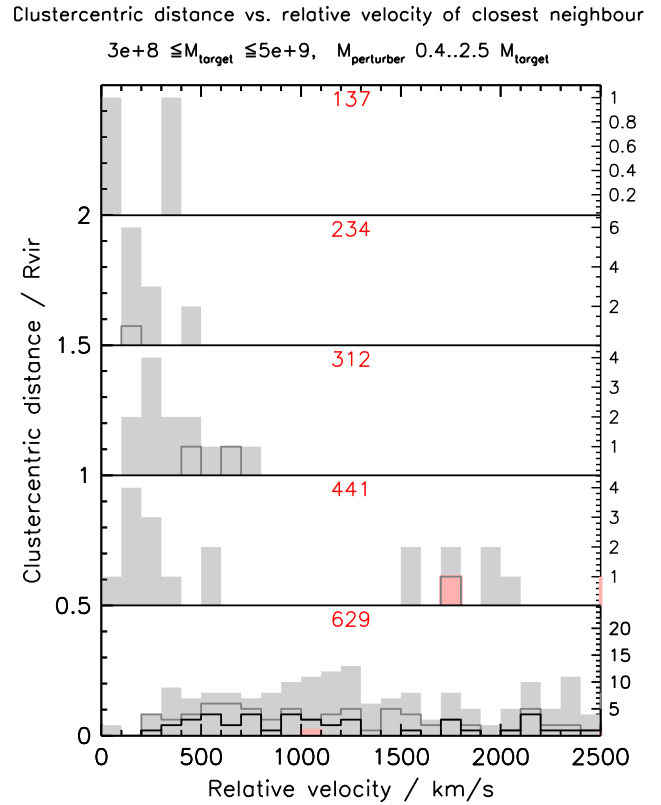


Fig. 6 (online colour at: www.an-journal.org) Distributions of relative velocity of the closest neighbour, for intervals in clustercentric distance and model clusters with $2.4 \times 10^{14} \leq M_{\text{vir}} \leq 4.0 \times 10^{14} M_{\odot}$. Number counts are given on the right. The pink shaded histogram indicates targets that have entered a larger halo not more than 3 Gyr ago. Further details as in Fig. 5.

Virgo cluster center with an artificial image of the model cluster with $M_{\text{vir}} = 3.1 \times 10^{14} M_{\odot}$, created with the same pixel scale and similar noise. The larger number of galaxies located close to the central galaxy in the model cluster is very obvious. Whether this is due to a shortcoming of the model or a peculiarity of the Virgo cluster itself still needs to be determined.

In addition to the above, it needs to be emphasized that $\sim 50\%$ of close passages in the model clusters actually take place in the close vicinity of a much more massive parent galaxy, whose tidal influence may be stronger than that of the respective neighbour. It would require dedicated N-body simulations to investigate what fraction of early-type dwarfs could exist relatively unperturbed close to a massive parent galaxy – for example, the Andromeda dE NGC 205 is known to be noticeably tidally perturbed by M31, but has also been found to display similar spiral structure as our objects of interest (Saviane et al. 2010).

Another relevant point is that spiral features can only be induced in galaxies that still have a dynamically cold stellar disk component. Low-mass galaxies whose disks have already been heated too much would be unlikely to show spiral structure. Therefore, it could be that significantly more

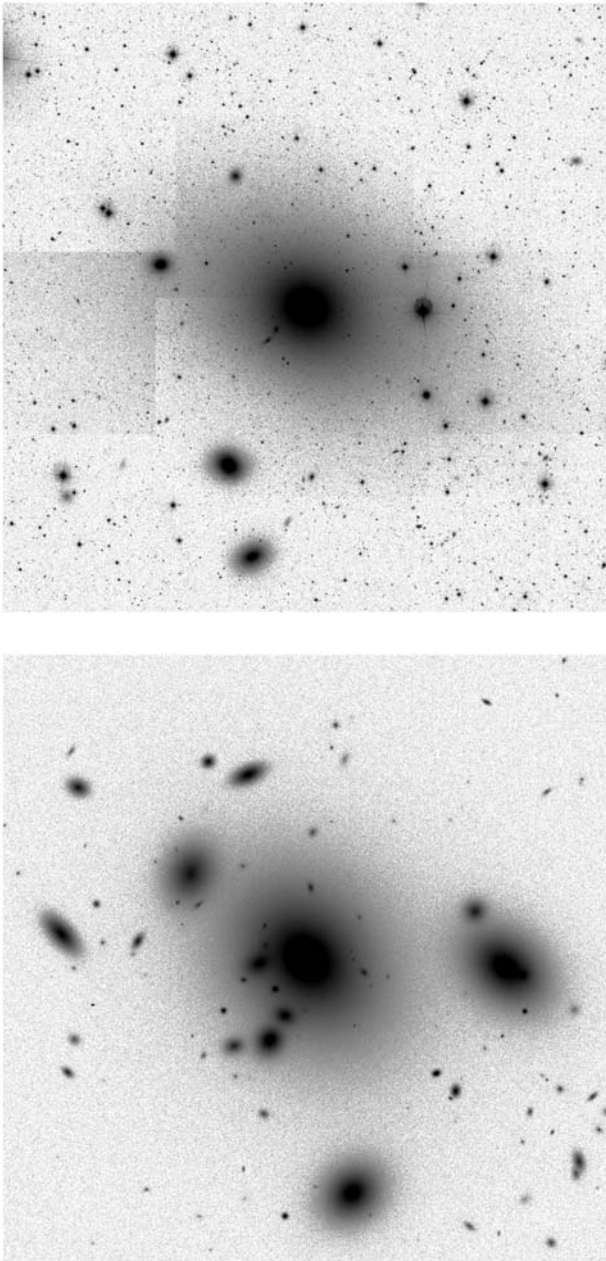


Fig. 7 Comparison of the Virgo cluster center around M87 (top, imaged with SDSS; North is right and East is up) to an artificial image of the model cluster with $M_{\text{vir}} = 3.1 \times 10^{14} M_{\odot}$, constructed to have similar noise and the same angular pixel size. The images are $30' \times 30'$ or $140 \times 140 \text{ kpc}^2$.

interactions would be needed to explain the observed number of spiral features, since only the fraction of galaxies with cold disks would show us observable signatures.

The conclusion from this section is that a non-negligible number of close interactions with low relative velocities do take place among dwarf galaxies in clusters, and that a certain fraction of the observed spirals and bars in early-type dwarfs is therefore likely to be caused by such interactions.

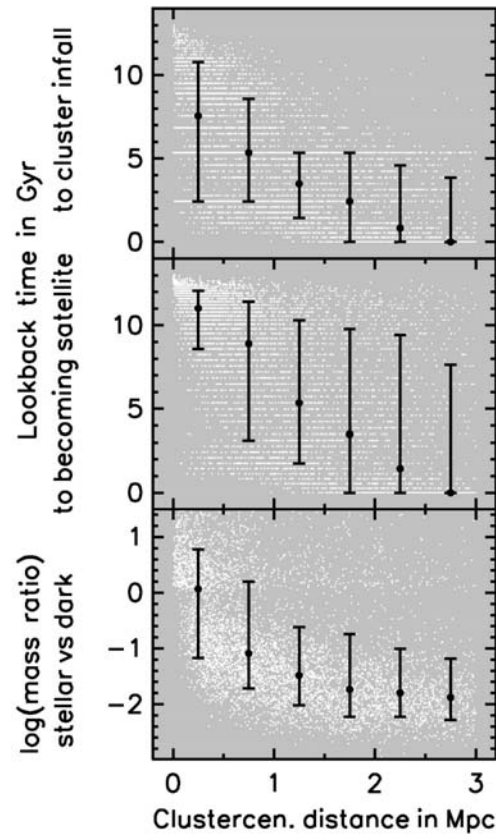


Fig. 8 Clustercentric distance of model galaxies versus quantities describing the infall and mass loss of subhalos. The ordinate of the *top panel* shows the lookback time to when a subhalo became a member of its present-day cluster halo. The lookback time to when a subhalo first became a satellite of any larger halo is shown in the *middle panel*. The *bottom panel* shows the stellar to dark matter mass ratio at $z = 0$. The sample encompasses galaxies with $-19.0 \leq M_r \leq -15.2 \text{ mag}$ from model clusters with virial masses between 1.4 and $4.0 \times 10^{14} M_{\odot}$ at redshift $z = 0$. For orphan galaxies, for which the subhalo mass had decreased below the resolution limit of 20 particles, a dark mass equal to 19 particles ($1.8 \times 10^8 M_{\odot}$) was adopted for the lower panel. Individual model galaxies are shown by white dots. Black circles and error bars denote the median and the $\pm 34\%$ range in intervals of 0.5 Mpc.

5 Mass loss and infall history

When low-mass galaxies, with their comparatively shallow potentials and low density, move through the galaxy cluster, the tidal forces exerted by the cluster potential and by close passages of other cluster members can partially or fully remove their dark matter halos. In the case that the dark matter mass drops below the resolution limit of the simulation, the remaining galaxies are dubbed “orphans”. Since the baryons are more concentrated than the dark matter, tidal stripping of the dark matter halo does not automatically mean that the stellar part of the galaxy gets disrupted. Nevertheless, a significant influence on the stellar configuration can be expected, but is not built into the models used (Guo et al. 2011).

Galaxies that have entered their host cluster halo at different epochs are – on average – located in different regions of the cluster today, as shown in Fig. 8 (top panel). In the range from 1.0 to 1.5 Mpc clustercentric distance, more than half of all galaxies have resided in the cluster since less than 4 Gyr, whereas in the very center, more than half have been in this cluster for longer than 7 Gyr. When considering the epoch at which a galaxy first became a satellite of a larger halo, then this has been even longer ago: more than 11 Gyr for the majority of cluster galaxies within the central 0.5 Mpc (Fig. 8 middle).

The ratio of stellar to dark mass can be used as indication for how strongly a galaxy has been affected by tidal forces: the dark matter subhalo is being stripped continuously while moving through the cluster. Fig. 8 (bottom) shows the strong correlation between stellar to dark mass ratio and location in the cluster. Galaxies in the cluster outskirts are still embedded in a massive dark matter halo, while a large fraction of galaxies in the center have already lost most of their dark matter. It is therefore worth distinguishing between cluster core and outskirts in the following.

The present-day ratio of total to stellar mass also correlates with the (three-dimensional) velocity with which a galaxy moves through the cluster core, as shown in Fig. 9 (top panel). This can probably be understood with the fact that slower galaxies spend, on average, a longer time in regions of strong tidal forces. In addition, velocity correlates with the time when a galaxy became a satellite, with later infall times leading to higher velocities on average. When considering projected quantities instead of three-dimensional ones (Fig. 9 bottom) the correlation is still clearly visible. Note that the correlation is largely determined by orphans, which are assigned a total to stellar mass ratio of 1 in the diagram.

When separating slow and fast galaxies at the median velocity value, their average mass ratios will thus be different, with fast galaxies having a larger ratio. In order to search for a correlation of the above effect with the assembly time of clusters, i.e. the lookback time to when they had acquired half of today's mass, Fig. 10 (top panel) shows the difference between the logarithmic mass ratios of slow and fast galaxies against this lookback time. This is done with projected quantities, i.e. using line-of-sight velocities and showing each cluster in three projections (different colours in the figure). The clusters have been assigned ID numbers from 1 to 15 in order of increasing mass, using clusters with $M_{\text{vir}} > 1.4 \times 10^{14} M_{\odot}$.

While no correlation with assembly time can be seen, the diagram is useful to illustrate the difference between the model clusters. The mass ratios of slow and fast galaxies can differ by as much as a factor 6, but can also be equal, depending on which cluster is chosen. Different projections of the same cluster often show significant differences in the mass ratios of slow and fast galaxies. In a few cases (e.g. cluster 10), fast galaxies can have lower mass ratios

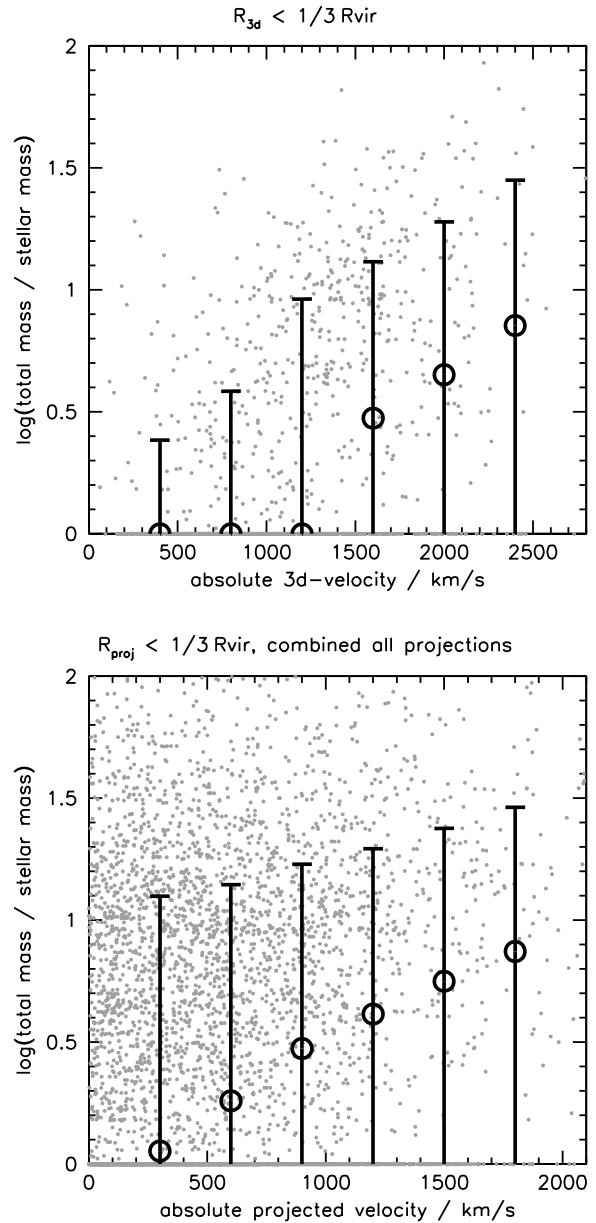


Fig. 9 *Top*: logarithm of total-to-stellar mass ratio versus velocity for galaxies with stellar mass between $3.0 \times 10^8 M_{\odot}$ and $5.0 \times 10^9 M_{\odot}$ and within $1/3$ virial radii from the cluster center, for model clusters with virial masses between 1.4 and $4.7 \times 10^{14} M_{\odot}$. Total mass is calculated from the database of Guo et al. (2011) as the sum of stellar mass and the product of subhalo particle number and particle mass, neglecting any remaining fraction of gas mass. Orphan (type 2) galaxies, which have completely lost their dark matter subhalo, get assigned a total mass that equals the stellar mass. Black circles denote median values in bins of velocity that are 800 km/s wide and placed every 400 km s^{-1} . Error bars denote the $\pm 34\%$ range of values. *Bottom*: same as top panel, but for projected clustercentric distance and line-of-sight velocity, showing data points from all projections. Bins are now 600 km s^{-1} wide and placed every 300 km s^{-1} .

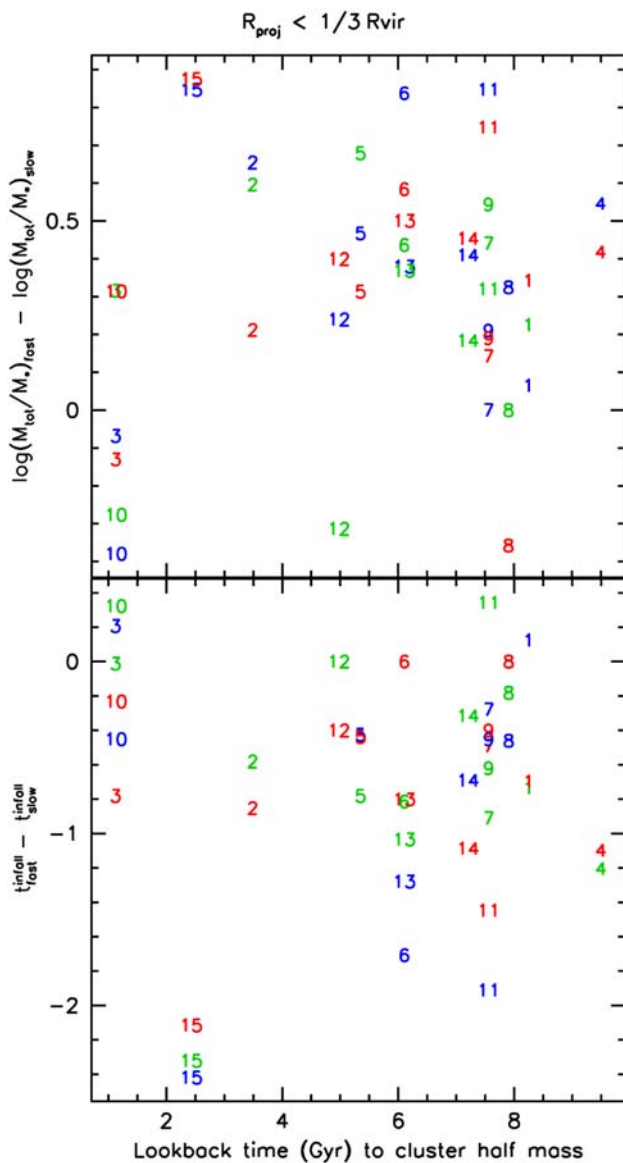


Fig. 10 (online colour at: www.an-journal.org) *Top*: difference between logarithmic total-to-stellar mass ratio of fast and slow galaxies versus lookback time to when a cluster had acquired 50% of today's mass. "Fast" and "slow" galaxies are distinguished at the median line-of-sight velocity of all galaxies, taking into account galaxies with stellar mass between $3.0 \times 10^8 M_{\odot}$ and $5.0 \times 10^9 M_{\odot}$ and within $1/3$ projected virial radii from the cluster center. The respective cluster IDs, sorted by increasing virial mass, are used instead of symbols; each projection is shown individually by different colours. *Bottom*: similar to top panel, but showing the difference between "infall time" of fast and slow galaxies. Infall time is the lookback time to when a galaxy had become a satellite.

than slow galaxies when viewed in one projection, but have higher mass ratios when viewed in another projection. This illustrates the difficulties in using observational signatures of galaxies of a given cluster to infer something about that specific cluster's evolutionary history and environmental influence.

Concerning the inclusion of orphan galaxies when analyzing mass ratios, it needs to be emphasized that the velocities and accurate positions of orphans may not be reliable. In the real universe, they may be affected by dynamical friction, especially since they are or were moving in regions of strong tidal forces (otherwise they would not have fully lost their dark matter halo). Nevertheless, this should only lead to lower velocities in most cases, thus regarding the current velocities as some kind of upper limit. Since most orphans already belong to the low-velocity part of the satellite population (Fig. 9), this would not change the overall picture. Furthermore, small changes in positions would not move the galaxy to a different regime of the cluster, thus not strongly affecting the statistics on galaxy populations.

Analogous to the difference in mass ratio between slow and fast galaxies (along the line of sight), Fig. 10 (bottom) shows that also a small but systematic difference in infall time exists. Here, infall time is taken to be the lookback time to when a galaxy became a satellite of a larger halo. This lookback time is somewhat larger for the slow galaxies than for the fast ones. Again, there is significant scatter between the model clusters and their different projections.

Different properties of fast and slow-moving dwarf galaxies in the cluster core are not only seen in the model universe. For nucleated dEs of the Virgo cluster, Lisker et al. (2009a) found a significant difference in galaxy shape between slow and fast ones: slow dEs have almost circular shapes, whereas fast dEs are significantly flatter. The investigation of model galaxies can thus help to interpret the observations: it seems likely that the stronger effect of tidal forces on the slow galaxies has led to a more substantial dynamical heating of those dEs, thus giving them their nearly circular shape. In this picture, the fast-moving dEs would be expected to be still rotationally flattened, having not yet experienced as much dynamical heating as the slow ones. Kinematical data that are currently being analyzed will confirm whether this interpretation is correct.

It is worth to point out that most of the above investigation does not rely on the particular choice of semi-analytic model ingredients, some of which may be debatable or need further fine-tuning. Instead, the motion of galaxies, the mass loss and disruption of their dark matter halos, and the dependence on infall time, all follow just from the underlying N-body simulation of matter and gravity. The semi-analytic model itself is "only" used here to be able to select galaxies by their stellar mass, and to define a total to stellar mass ratio. The presented correlations of the model quantities can thus be considered as predictions from dark matter subhalo distributions and motions, and the observational study of Virgo cluster dwarfs can be seen as a method to trace these subhalos by observations, confirming the predictions.

6 Disruption of dwarfs

The semi-analytic model of Guo et al. (2011) includes a criterion for when a satellite galaxy – including its stellar body

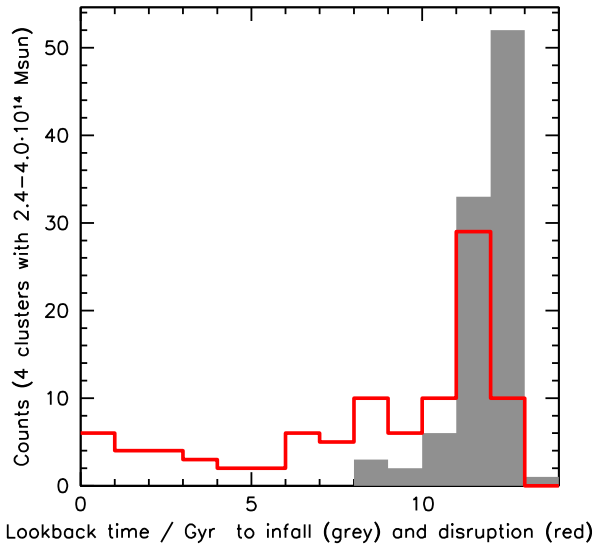


Fig. 11 (online colour at: www.an-journal.org) Lookback time to disruption of model galaxies (red) and previous infall of those galaxies into a larger halo (grey), for galaxies in the stellar mass range $3 \times 10^8 \leq M_* \leq 5 \times 10^9 M_\odot$. Model clusters with $2.4 \times 10^{14} \leq M_{\text{vir}} \leq 4.0 \times 10^{14} M_\odot$ are considered.

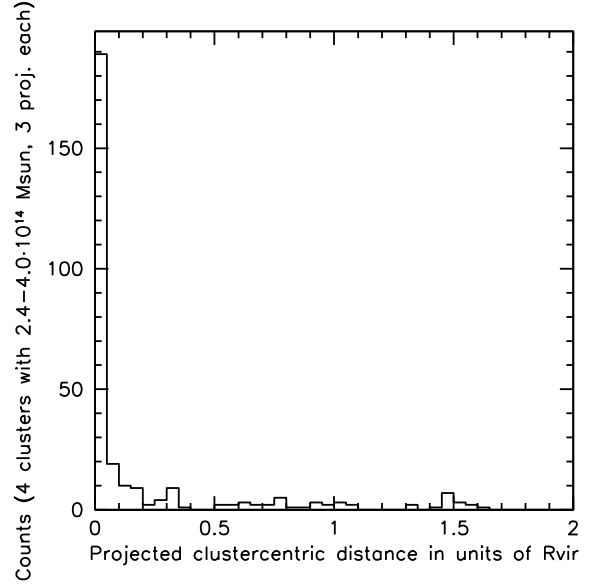


Fig. 12 Present-day projected clustercentric distance of those halos containing the remnants from the disruption events shown in Fig. 11, again for clusters with $2.4 \times 10^{14} \leq M_{\text{vir}} \leq 4.0 \times 10^{14} M_\odot$. All three projections of each cluster are included in the diagram.

– gets completely disrupted. This happens when the average baryonic mass density within the half-mass radius of the satellite is lower than the average mass density of the parent halo within the pericentric distance (Eq. 30 of Guo et al. 2011). If this criterion is fulfilled, the stars of the galaxy are instantaneously assigned to the population of intracluster/group stars. Although not simulated or modeled, it can be assumed that a nucleus, i.e. a compact stellar cluster at the core of the disrupted galaxy, could survive this process and remain as a UCD.

To estimate from the model how many disruptions of potentially nucleated galaxies happened in the past of a cluster, I focus on the stellar mass range $3 \times 10^8 \leq M_* \leq 5 \times 10^9 M_\odot$, roughly corresponding to a range of $-16.3 \leq M_r \leq -18.6$ mag in absolute magnitude. Most early-type dwarf galaxies in this range possess a compact stellar nucleus of significant luminosity, i.e. beyond that of an ordinary globular cluster. In the Virgo cluster, there are 280 galaxies of all types in this magnitude range (Weinmann et al. 2011), 84 of which are nucleated early-type dwarfs. 18 galaxies are spirals of type Sd, which often host nuclei that are similar in size and mass to those of the early-type dwarfs (Böker et al. 2002, 2004). I thus assume that 100 out of 280 galaxies, or 36 %, could serve as UCD progenitors.

The Guo et al. (2011) database yields galaxies in the above stellar mass range that are being disrupted at any epoch, and whose parent halo ends up in a given cluster today. The distributions of the lookback time to disruption, as well as the lookback time to becoming a satellite, are shown in Fig. 11 for the four model clusters with

$2.4 \times 10^{14} \leq M_{\text{vir}} \leq 4.0 \times 10^{14} M_\odot$. Obviously, most disruption processes happened at very early times, ~ 10 Gyr ago. Furthermore, even for those galaxies that were disrupted more recently, infall into a larger halo occurred at least 7 Gyr ago.

The four model clusters altogether host the remnants of 97 disrupted galaxies. Dividing by 4 and multiplying by the above nucleated fraction of 0.36 leads to a number of 9 potentially surviving nuclei per cluster. These objects are mostly located in the very cluster core, as show in Fig. 12. Either the majority of disruptions occurred in the vicinity of the central cluster galaxy, or the halos in which the disruptions took place merged with it. Considering that 78% of the potential remnants are found within a projected clustercentric distance of $0.2R_{\text{vir}}$, 7 UCDs are predicted within $0.2 \times 1.5 = 0.3$ Mpc of the Virgo cluster center, marked by M87.

The true number of UCDs in the Virgo cluster core is difficult to pin down, both due to the identification process (basically a point source with a redshift compatible with being a cluster member) and the uncertain distinction between a massive globular cluster of M87 and a “real” stripped-nucleus UCD. Evstigneeva et al. (2005) and Jones et al. (2006) list 9 Virgo UCDs; another detection was reported by Paudel et al. (2010). Note that these objects are relatively bright ($M_r < -11.5$ mag), as a consequence of them being “confirmed” UCDs — otherwise they would be counted only as candidates due to the larger brightness overlap with globular clusters.

The number of 7 expected UCDs might appear nicely consistent with the 10 confirmed Virgo UCDs from the studies mentioned above. However, the distribution of nucleus and UCD magnitudes (Paudel et al. 2010) implies that only about one third of nuclei are sufficiently bright to count as clear, unambiguous UCD, leading to only 2 expected objects from the models. This obviously leaves room for discussion concerning both the real and the model universe: Weinmann et al. (2011) have argued that disruption of dwarf galaxies may still be too inefficient in the model, and they found a dwarf-to-giant ratio that was systematically too high in the model by a factor of two. While this could partly alleviate the discrepancy, an alternative explanation could be that a number of UCDs are formed by a different process, e.g. by the merging of super star clusters (Fellhauer & Kroupa 2005).

By restricting the analysis to the stellar mass range of $3 \times 10^8 \leq M_* \leq 5 \times 10^9 M_\odot$ for the disrupted objects, additional “UCDs” of the model might have been excluded. However, the number of galaxies per mass interval steeply decreases towards higher masses, and in addition they are increasingly more difficult to disrupt. At lower masses, the nucleated fraction decreases, and the chance to find a nucleus as bright as the confirmed UCDs gets very low, as they contain not more than $\sim 10\%$ of the galaxy light (Binggeli et al. 2000). The above approach should therefore capture more than 50% of those objects that would end up as today’s UCDs after disruption of their host galaxy. Naturally, an evolutionary caveat persists: it is not known whether nuclei at earlier epochs were different in their properties, e.g. brighter or more frequent than today.

Given that ram pressure stripping and tidal stripping affect the cold gas reservoir of low-mass satellites, the early infall into a larger halo for all galaxies that are later disrupted implies that none of the potential remnants should contain a noticeable young stellar population. This is consistent with the observational finding that all UCDs show old stellar population ages (Paudel et al. 2010).

This investigation, though relying on many assumptions and simplifications, illustrates how the model universe can provide insight into the history of observed galaxies in our nearby universe. Future models with improved treatment of disruption processes, together with future observations of UCDs in more distant galaxy clusters, could then lead to using UCDs, their properties, abundance, and distribution, as witnesses of the early phase of galaxy clusters.

7 Conclusions

As astronomical observers, we only have a restricted view of the positions and motion of galaxies. Therefore, the “model universe” represented by the high-resolution Millennium-II cosmological simulation (Boylan-Kolchin et al. 2009) and the state-of-the-art semi-analytic model of Guo et al. (2011) can serve as valuable tool to obtain a six-dimensional view of galaxy populations. If the overall char-

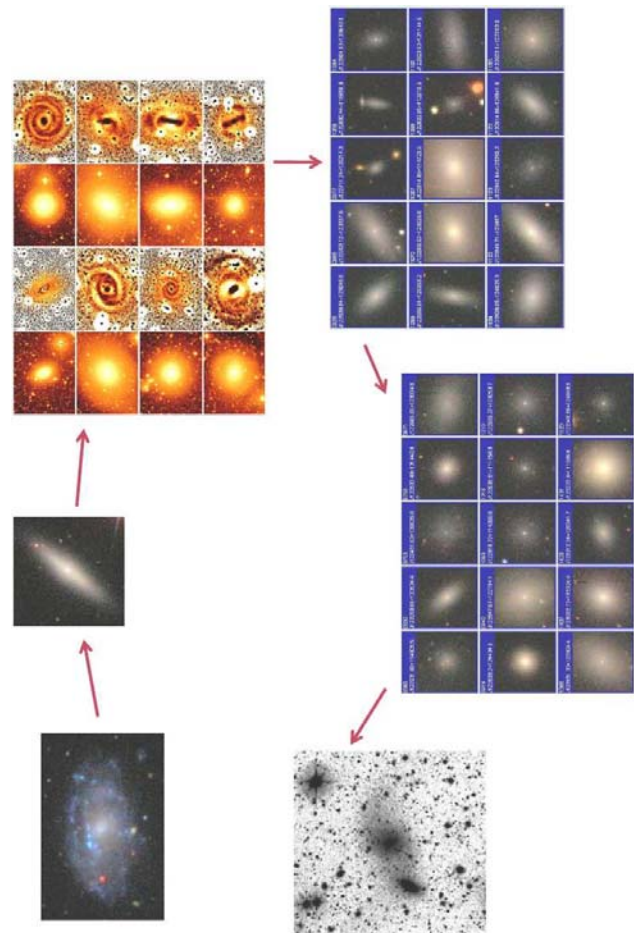


Fig. 13 Illustration of the possible stages a low-mass cluster galaxy goes through. Given that the images are actually showing galaxies *at present*, the arrows can also be considered to indicate the direction of increasing lookback time to when these galaxies entered the cluster.

acteristics of galaxies and clusters in the model appear to be in agreement with our real universe, in a statistical sense, then one can perform similar selections of galaxy samples in both universes, and compare the restricted observer’s view to the comprehensive modeler’s view of “the same” galaxies.

Observations revealed that Virgo cluster early-type galaxies moving faster along the line of sight with respect to the systemic velocity of the cluster exhibit shapes that are significantly less round than those of slower-moving galaxies (Lisker et al. 2009a). In the model universe, those galaxies in the slow subsample lost more (up to all) of their dark matter subhalos, indicating that they were affected more strongly by tidal forces over time. This leads to the interpretation that dynamical heating has been responsible for the nearly round galaxy shapes of the slow-moving galaxies.

Tidal disruptions of low-mass galaxies mostly occurred many gigayears ago in the model, and all these had become satellites of a larger halo already at early epochs. This is in good agreement with the old stellar populations of UCDs in

the Virgo cluster Paudel et al. (2010), provided that they are remnant nuclei from disrupted galaxies.

The variety of early-type dwarf galaxy characteristics, with various subclasses showing different shapes, spatial distributions and stellar population properties, had led us to conclude that there must be different formation channels at work to form them (Lisker et al. 2007). However, the comparison to the model galaxies indicates that a simpler solution may exist when all circumstances are considered: Those low-mass late-type galaxies that have fallen into the cluster only within the past few gigayears predominantly have more eccentric orbits and larger velocities than those low-mass galaxies residing in the cluster core since long time. While still losing their gas due to ram-pressure stripping, these orbits will prevent them from strong tidal heating and “harassment”, and at the same time, the comparably long time they spend in the cluster outskirts causes them to take part in galaxy interactions. Thus, in contrast to their relatives who spend more time deeper inside the cluster potential, they have a somewhat younger average stellar population, a flatter shape, and tidally triggered spiral features and bars, making them appear as a distinct subpopulation to observers.

Figure 13 illustrates the different stages that a low-mass galaxy may go through, following the picture outlined above. However, instead of considering this to be one sequence of events, it is rather the case that different galaxies today are in different stages of this evolution, and therefore contribute different subpopulations to the cluster dwarf galaxies. Most disruption remnants in today’s clusters come from early events, and also the subpopulation of round, slow-moving dEs in the cluster core has probably entered at early epochs. Thus, going in the *reverse* direction of Fig. 13 leads to more recent infall into the cluster, ending with today’s low-mass late-type galaxies that are just about to feel the influence of the cluster environment for the first time.

Acknowledgements. I would like to warmly thank Eva Grebel for her continuous support. My thanks also go to Simone Weimann, Joachim Janz, and Hagen Meyer for their contributions to part of the research presented here. I am supported within the framework of the Excellence Initiative by the German Research Foundation (DFG) through the Heidelberg Graduate School of Fundamental Physics (grant number GSC 129/1). This work is partly based on the SDSS, for which funding has been provided by the Alfred P. Sloan Foundation, the Participating Institutions, the National Science Foundation, the U.S. Department of Energy, the National Aeronautics and Space Administration, the Japanese Monbukagakusho, the Max Planck Society, and the Higher Education Funding Council for England. The SDSS Web Site is <http://www.sdss.org/>.

References

Abazajian, K.N., et. al.: 2009, *ApJS* 182, 543
Bender, R., Nieto, J.-L.: 1990, *A&A* 239, 97

Binggeli, B., Popescu, C.C.: 1995, *A&A* 298, 63
Binggeli, B., Sandage, A., Tammann, G.A.: 1985, *AJ* 90, 1681
Binggeli, B., Barazza, F., Jerjen, H.: 2000, *A&A* 359, 447
Binney, J.: 1978, *MNRAS* 183, 501
Böker, T., Laine, S., van der Marel, R.P., Sarzi, M., Rix, H., Ho, L.C., Shields, J.C.: 2002, *AJ* 123, 1389
Böker, T., Sarzi, M., McLaughlin, D.E., van der Marel, R.P., Rix, H., Ho, L.C., Shields, J.C.: 2004, *AJ* 127, 105
Boselli, A., Boissier, S., Cortese, L., Gavazzi, G.: 2008, *ApJ* 674, 742
Boylan-Kolchin, M., Springel, V., White, S.D.M., Jenkins, A., Lemson, G.: 2009, *MNRAS* 398, 1150
Chiboucas, K., Tully, R.B., Marzke, R.O., et al.: 2011, *ApJ* 737, 86
Chilingarian, I.V.: 2009, *MNRAS* 394, 1229
De Rijcke, S., Michielsen, D., Dejonghe, H., Zeilinger, W.W., Hau, G.K.T.: 2005, *A&A* 438, 491
Evstigneeva, E.A., Gregg, M.D., Drinkwater, M.J.: 2005, in: H. Jerjen, B. Binggeli (eds.), *Near-field cosmology with dwarf elliptical galaxies*, IAU Coll. 198, p. 413
Fellhauer, M., Kroupa, P.: 2005, *MNRAS* 359, 223
Guo, Q., et al.: 2011, *MNRAS* 413, 101
Hilker, M., Infante, L., Vieira, G., Kissler-Patig, M., Richtler, T.: 1999, *A&AS* 134, 75
Janz, J., Lisker, T.: 2008, *ApJ* 689, L25
Janz, J., Laurikainen, E., Lisker, T., et al.: 2012, *ApJ* 745, L24
Jones, J.B., Drinkwater, M.J., Jurek, R., et al.: 2006, *AJ* 131, 312
Lisker, T.: 2011, Habilitation Thesis, Universität Heidelberg
Lisker, T., Fuchs, B.: 2009, *A&A* 501, 429
Lisker, T., Grebel, E.K., Binggeli, B., Glatt, K.: 2007, *ApJ* 660, 1186
Lisker, T., Janz, J., Hensler, G., et al.: 2009a, *ApJ* 764, L124
Lisker, T., Brunngräber, R., Grebel, E.K.: 2009b, *AN* 330, 966
Mastropietro, C., Moore, B., Mayer, L., et al.: 2005, *MNRAS* 364, 607
Moore, B., Katz, N., Lake, G., Dressler, A., Oemler, A.: 1996, *Nature* 379, 613
Paudel S., Lisker T., Janz J.: 2010, *ApJ* 724, L64
Pedraz, S., Gorgas, J., Cardiel, N., Sánchez-Blázquez, P., Guzmán, R.: 2002, *MNRAS* 332, L59
Petropoulou, V., Vílchez, J., Iglesias-Páramo, J., et al.: 2011, *ApJ* 734, 32
Sandage, A., Binggeli, B.: 1984, *AJ* 89, 919
Saviane, I., Monaco, L., Hallas, T.: 2010, in: G. Bruzual, S. Charlot (eds.), *Stellar populations – planning for the next decade*, IAU-Symp. 262, p. 426
Schindler, S., Binggeli, B., Böhringer, H.: 1999, *A&A* 343, 420
Simien, F., Prugniel, P.: 2002, *A&A* 384, 371
Smith, R., Davies, J.I., Nelson, A.H.: 2010, *MNRAS* 405, 1723
Toloba, E., Boselli, A., Gorgas, J., et al.: 2009, *ApJ* 707, L17
Toloba, E., Boselli, A., Cenarro, A.J., et al.: 2011, *A&A* 526, A114
Torres-Flores, S., Mendes de Oliveira, C., de Mello, D.F., et al.: 2009, *A&A* 507, 723
Tully, R.B., Trentham, N.: 2008, *AJ* 135, 1488
Tutukov, A.V., Fedorova, A.V.: 2006, *Astronomy Reports* 50, 785
Weinmann, S.M., Lisker, T., Guo Q., Meyer, H.T., Janz, J.: 2011, *MNRAS* 416, 1197
White, S.D.M., Briel, U.G., Henry, J.P.: 1993, *MNRAS* 261, L8
van Zee, L., Skillman, E.D., Haynes, M.P.: 2004, *AJ* 128, 121